



Contents lists available at ScienceDirect

Saudi Journal of Biological Sciences

journal homepage: www.sciencedirect.com

Original article

In silico screening of FDA approved drugs reveals ergotamine and dihydroergotamine as potential coronavirus main protease enzyme inhibitors

Arun Bahadur Gurung^{a,*}, Mohammad Ajmal Ali^b, Joongku Lee^{c,*}, Mohammad Abul Farah^d, Khalid Mashay Al-Anazi^d^a Department of Basic Sciences and Social Sciences, North-Eastern Hill University, Shillong 793022, Meghalaya, India^b Department of Botany and Microbiology, College of Science, King Saud University, Riyadh 11451, Saudi Arabia^c Department of Environment and Forest Resources, Chungnam National University, 99 Daehak-ro, Yuseong-gu, Daejeon 34134, Republic of Korea^d Genetics Laboratory, Department of Zoology, College of Science, King Saud University, Riyadh 11451, Saudi Arabia

ARTICLE INFO

Article history:

Received 2 May 2020

Revised 30 May 2020

Accepted 3 June 2020

Available online 10 June 2020

Keywords:

Coronaviruses
Coronaviral main protease
FDA approved drugs
Ergotamine
Dihydroergotamine
COVID-19
SARS-CoV-2
SARS-CoV
MERS-CoV
2019-nCoV

ABSTRACT

Coronaviruses with the largest viral genomes are positive-sense RNA viruses associated with a history of global epidemics such as the severe respiratory syndrome (SARS), the Middle East respiratory syndrome (MERS) and recently the coronavirus disease 2019 (COVID-19). There has been no vaccines or drugs available for the treatment of human coronavirus infections to date. In the present study, we have explored the possibilities of FDA approved drugs as potential inhibitors of the coronavirus main protease, a therapeutically important drug target playing a salient role in the maturation and processing of the viral polyproteins and are vital for viral replication and transcription. We have used molecular docking approach and have successfully identified the best lead molecules for each enzyme target. Interestingly, the anti-migraine drugs such as ergotamine and its derivative, dihydroergotamine were found to bind to all the three target enzymes within the Cys-His catalytic dyad cleft with lower binding energies as compared to the control inhibitors (α -ketoamide 13b, SG85 and GC813) and the molecules are held within the pocket through a good number of hydrogen bonds and hydrophobic interactions. Hence both these lead molecules can be further taken for wet-lab experimentation studies before repurposing them as anti-coronaviral drug candidates.

© 2020 The Author(s). Published by Elsevier B.V. on behalf of King Saud University. This is an open access article under the CC BY-NC-ND license (<http://creativecommons.org/licenses/by-nc-nd/4.0/>).

1. Introduction

Coronaviruses are enveloped positive-sense RNA viruses which have crown-like appearance under the electron microscope and usually ranges from 60 to 140 nm in diameter (Richman et al., 2016). There are four coronaviruses (OC43, 229E, NL63 and HKU1) which cause mild respiratory distress in humans (Singhal, 2020). The cross-species transmission of animal beta coronaviruses to humans have been reported since last two decades-the first

event which occurred in 2002–2003 when the bat originated coronaviruses crossed over to humans via palm civet cats as intermediary host and caused severe respiratory syndrome (SARS) in humans and was known as SARS coronaviruses (SARS-CoV) which infected 8422 people in China and Hong Kong and caused 916 deaths with a mortality rate of 11% (Chan-Yeung and Xu, 2003). In 2012, almost a decade later, another bat-originated virus emerged in Saudi Arabia and the transmission to humans was via dromedary camels. The virus was designated as the Middle East respiratory syndrome coronavirus (MERS-CoV) which infected 2494 people and caused 858 deaths with fatality rate of 34% (Singhal, 2020). There is a recent global health emergency around the world with the rapid emergence and spread of 2019 novel coronavirus (2019-nCoV) or the severe acute respiratory syndrome coronavirus 2 (SARS-CoV-2) which has caused a pandemic known as coronavirus disease 2019 (COVID-19). The outbreak was first reported in Wuhan, Hubei province, China in December 2019 (Wang et al., 2020). The intermediary hosts which led to the transmission of this

* Corresponding authors.

E-mail addresses: arunbgurung@gmail.com (A.B. Gurung), joongku@cnu.ac.kr (J. Lee).

Peer review under responsibility of King Saud University.



Production and hosting by Elsevier

<https://doi.org/10.1016/j.sjbs.2020.06.005>

1319-562X/© 2020 The Author(s). Published by Elsevier B.V. on behalf of King Saud University.

This is an open access article under the CC BY-NC-ND license (<http://creativecommons.org/licenses/by-nc-nd/4.0/>).

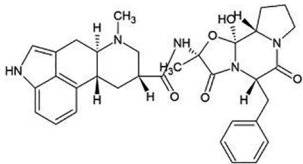
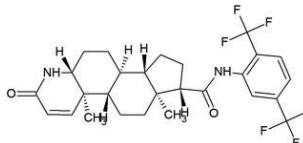
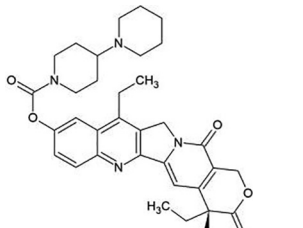
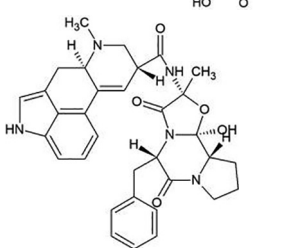
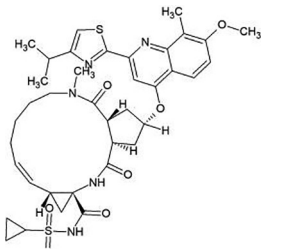
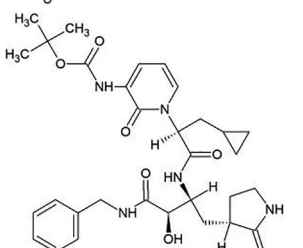
bat-originated virus to humans is still an enigma. According to the WHO report, there has been 25,49,632 confirmed cases of COVID-19 and 1,75,825 confirmed deaths to date (23/04/2020) (Coronavirus disease Pandemic, 2020).

The coronaviruses (CoVs) RNA genome has a size ranging from 27 to 31 kb and it is the largest viral RNA genomes known to date (Lai and Holmes, 2001). The two overlapping polyproteins (pp1a and pp1ab) encoded by the CoV replicase gene are essential for viral replication and transcription (Snijder and Spaan, 1995; Yang et al., 2003). These polyproteins need to undergo a complex cascade of proteolytic processing for maturation which in turn

regulates viral gene expression and replication (Xue et al., 2008). The enzyme CoV main protease (CoV M^{Pro}; also known as 3C-like protease or 3CL^{Pro}) catalyzes the most of the maturation cleavage events within the precursor polyproteins (Lee et al., 1991; Ziebuhr et al., 2000). It is a three-domain (domains I to III) cysteine protease with a chymotrypsin-like fold at the N terminus and a Cys-His catalytic located in a cleft between domains I and II (Anand et al., 2003; Yang et al., 2003). The CoV M^{Pro} has emerged as an attractive drug target for anti-coronaviral drug design because of its vital role in the maturation and processing of the replicase polyprotein (Xue et al., 2008; Ziebuhr et al., 2000). The

Table 1

Binding energy scores and molecular interactions between top 5 leads and SARS-CoV-2 M^{Pro}. The figures in bracket indicate the hydrogen bond length.

ZINC ID	Common Name	Structure	Binding Energy (kcal/mol)	Molecular Interactions	
				Hydrogen bonds	Hydrophobic interactions
ZINC000003978005	Dihydroergotamine		-9.4	O1.....N(Gly143) [3.13 Å] O4.....N(Gly143) [2.80 Å]	Thr25, His41, Cys44, Met49, Asn142, Cys145, His164, Met165 and Glu166 (N = 9)
ZINC000003932831	Avodart		-9.3	N1.....O(Gln192) [3.29 Å] F3.....NE2(His163) [3.07 Å]	Leu141, Asn142, Gly143, Cys145, Met165, Glu166, Pro168, Arg188, Gln189 and Thr190 (N = 10)
ZINC000001612996	Irinotecan		-9.3	N4.....O(Thr26) [3.00 Å] O3.....NE2(Gln192) [2.90 Å]	Thr24, Thr25, His41, Met49, Asn119, Gly143, Cys145, His164, Met165, Glu166, Pro168, Gln189 and Thr190 (N = 13)
ZINC000052955754	Ergotamine		-9.3	O4.....N(Gly143) [3.13 Å]	Thr25, His41, Cys44, Met49, Asn142, Cys145, His164, Met165, Glu166, Asp187 and Arg188 (N = 11)
ZINC000164760756	Olysiso		-9.2	O6.....OG1 (Thr25) [2.94 Å]	His41, Cys44, Thr45, Ser46, Met49, Phe140, Leu141, Asn142, Gly143, His163, His164, Met165, Glu166, Gln189 and Thr190 (N = 15)
Control (O6K)	α -ketoamide 13b		-6.9	O26.....NE2(His41) [3.10 Å] O37.....N(Glu1660) [3.23 Å]	Thr25, Met49, Cys145, His163, Met165, Pro168, Gln189 and Thr190 (N = 8)

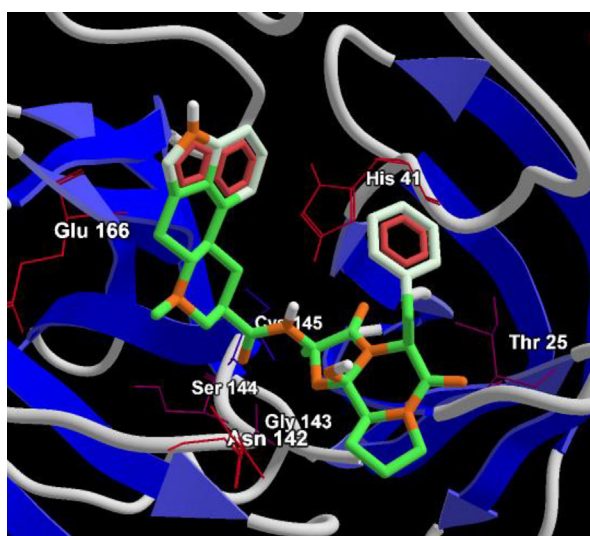
enzyme has been targeted previously with antiviral phytochemicals (Gurung et al., 2020; Islam et al., 2020; Tahir ul Qamar et al., 2020), marine natural products (Gentile et al., 2020) and FDA approved drugs (Kandeel and Al-Nazawi, 2020; Lobo-Galo et al., 2020).

The lack of effective therapeutics against human coronaviral infections (Graham et al., 2013) and the high mortality rates due to the recent emergence of novel coronavirus (2019-nCoV) have necessitated the discovery of new vaccines or drugs. In the present study, we have explored the possibility of the FDA approved drugs as potential inhibitors of M^{Pro} enzyme which will help in halting the virus replication and curtail the progression of the disease. We have used molecular docking study to explore the binding interaction of the FDA approved drugs with three target enzymes (SARS-CoV M^{Pro} , SARS-CoV-2 M^{Pro} and MERS-CoV M^{Pro}) and short-listed suitable lead molecules for each target.

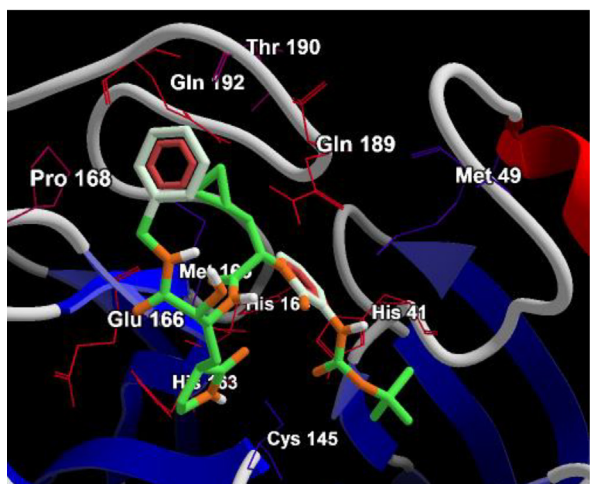
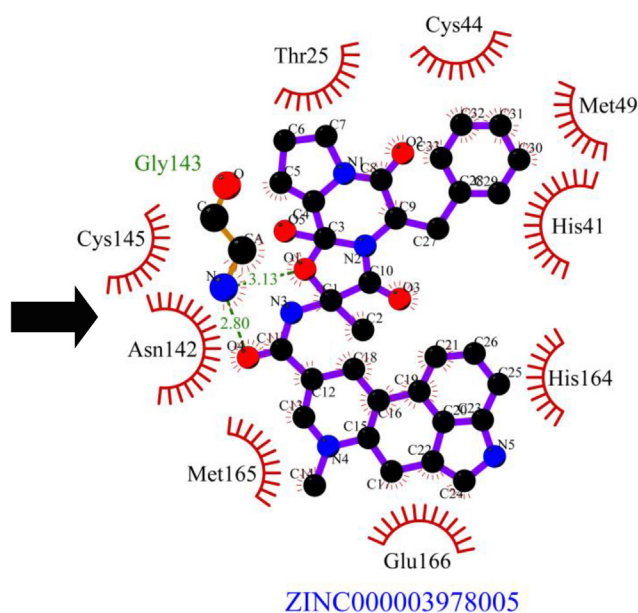
2. Materials and methods:

2.1. Retrieval and preparation of structures of FDA approved drugs:

A set of 1390 chemical structures of FDA approved drugs were downloaded from ZINC 15 database (Sterling and Irwin, 2015). The 3D structures of the molecules in SDF format were retrieved and the molecules having only 2D structure available were processed into 3D structures using Open Babel version 2.4.1 software (O'Boyle et al., 2011) and subsequently energy-optimized using MMFF force field (Halgren, 1996) following our previously described protocol (Gurung et al., 2016). The molecules were prepared for docking using AutoDock Tools-1.5.6 by the addition of Gasteiger charges and hydrogen atoms and torsions for each molecule were optimally defined. The structures of the compounds were saved in PDBQT format.



(A)



(B)

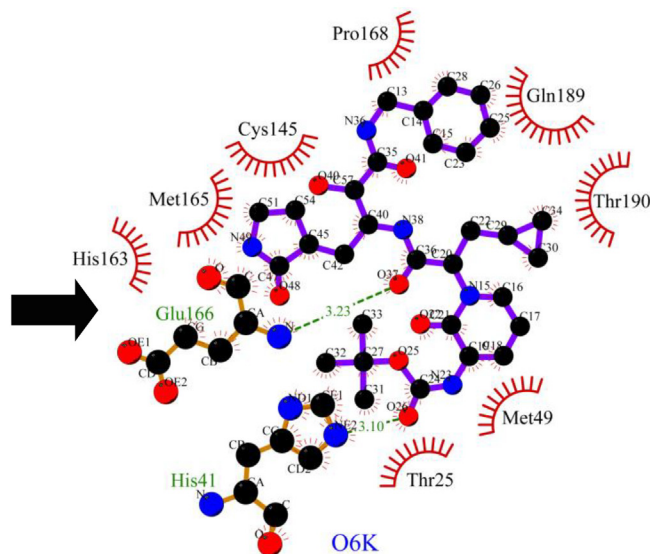
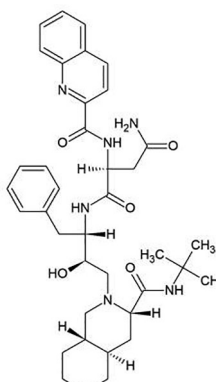
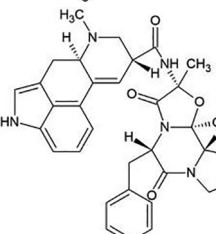
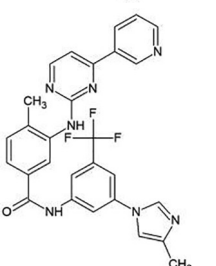
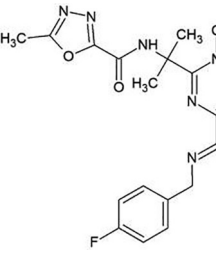
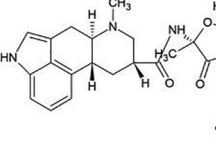
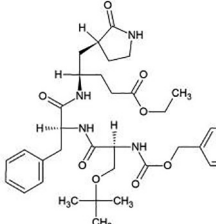


Fig. 1. Binding conformation (compounds are represented as green sticks and key interacting residues are displayed in thin red wireframe representation) and molecular interaction between SARS-CoV-2 M^{Pro} and (A) Dihydroergotamine (ZINC00003978005) (B) α -ketoamide 13b inhibitor (O6K). The hydrophobic interactions are indicated by red arcs with radiating spikes and green dashed lines correspond to hydrogen bonds.

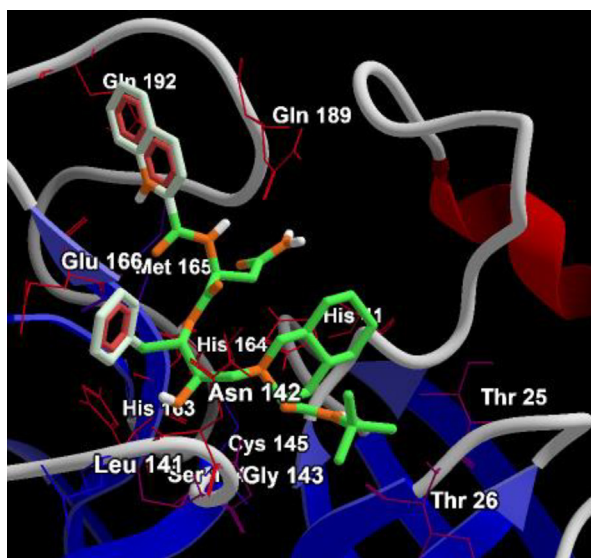
Table 2Binding energy scores and molecular interactions between top 5 leads and SARS-CoV M^{Pro}. The figures in bracket indicate the hydrogen bond length.

ZINC ID	Common Name	Structure	Binding Energy (kcal/mol)	Molecular Interactions	
				Hydrogen bonds	Hydrophobic interactions
ZINC000026985532	Saquinavir		-9.6	O6.....N(Glu166) [2.83 Å] N5.....OE1(Gln189) [3.06 Å] O2.....O(Leu141) [2.75 Å] O1.....N(Gly143) [2.89 Å]	Thr25,Thr26, His41,Met49, Phe140, Asn142, Cys145, His164, Met165, Leu167, Thr190 and Gln192 (N = 12)
ZINC000052955754	Ergotamine		-9.5	O1.....N(Gly143) O4.....N(Gly143)	Thr25, His41, Met49, Asn142, Cys145, His164, Met165, Glu166 and Gln189 (N = 9)
ZINC000006716957	Nilotinib		-9.4	N4.....OD(Asn142) [3.03 Å] N1.....O(His164) [3.15 Å]	Thr25, His41, Cys44, Met49, Phe140, Cys145, His163, Met165, Glu166 and Gln189 (N = 10)
ZINC000013831130	Raltegravir		-9.2	O4.....O(His41) [2.95 Å] O2.....N(Cys145) [3.25 Å] N5.....OD1 (Asn142) [2.83 Å]	Thr25, Thr26, Leu27, Cys44, Met49, Leu141, Gly143, Asp187, Arg188 and Gln189, (N = 10)
ZINC000003978005	Dihydroergotamine		-9.2	O4.....N(Ser144) [3.34 Å] O4.....N(Gly143) [2.67 Å] O1.....N(Gly143) [2.98 Å]	Thr25, Leu27, His41, Cys44, Met49, Asn142, Cys145, His164, Met165, Glu166 and Gln189 (N = 11)
Control (G85)	SG85		-7.9	O19.....N(Cys145) [3.20 Å] O19.....SG(Cys145) [3.28 Å] N49.....OE1(Gln189) [2.89 Å] O47.....N(Glu166) [3.02 Å]	Thr25, Thr26, His41, Met49, Phe140, Leu141, Asn142, Gly143, Ser144, His163, His164, Met165, Asp187, Thr190, Ala191 and Gln192 (N = 16)

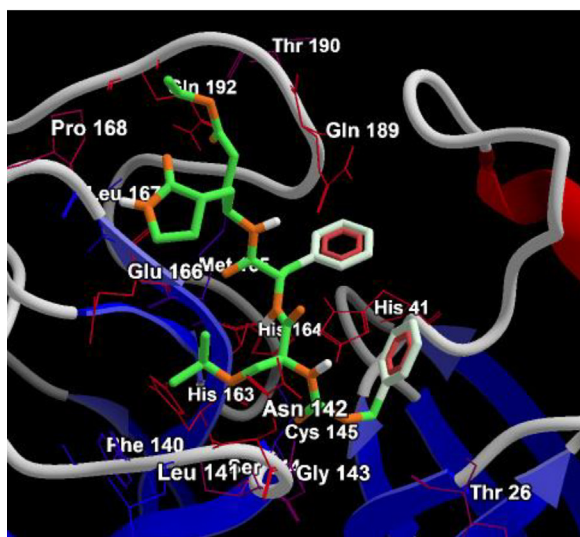
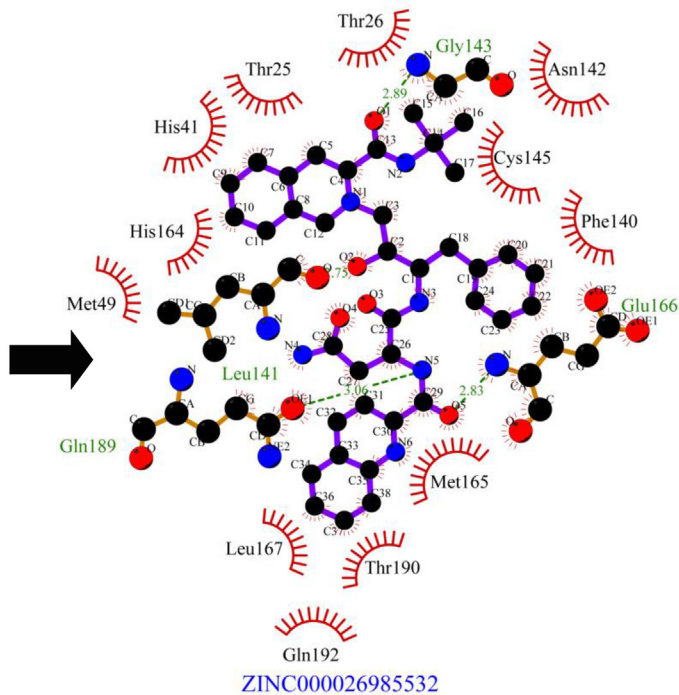
2.2. Retrieval and preparation of structures of target enzymes

The three-dimensional structures of the enzyme targets-SARS-CoV-2 M^{Pro} (PDB ID: 6Y2F), SARS-CoV M^{Pro} (PDB ID: 3TNT) and MERS-CoV M^{Pro} (PDB ID: 5WKK) solved through high-resolution X-ray crystallographic technique at a resolution of 1.95 Å, 1.59 Å and 1.55 Å respectively were retrieved from Protein Data Bank

(<http://www.rcsb.org/>). Each target enzyme was prepared by removing the heteroatoms including ions, co-crystallized ligands (O6Y, G85 and AW4 corresponding to PDB IDs: 6Y2F, 3TNT and 5WKK respectively) and water molecules. Further, an optimum number of polar hydrogen atoms and Kolmann charges were added to each protein target using AutoDock Tools-1.5.6 and the structures were saved in PDBQT format.



(A)



(B)

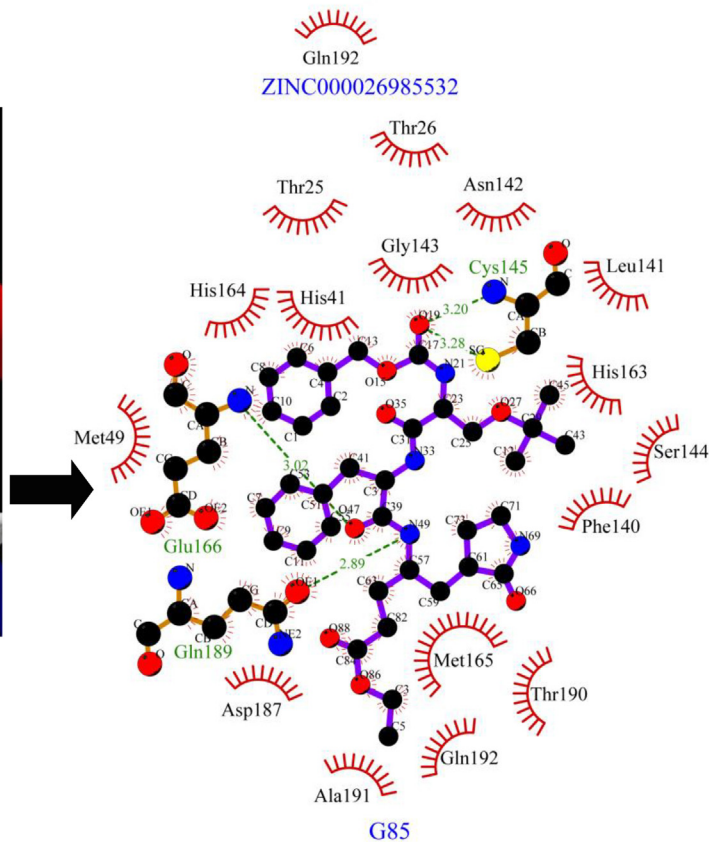


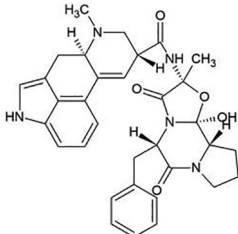
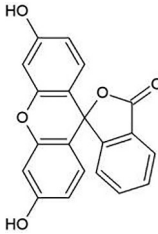
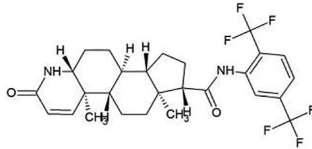
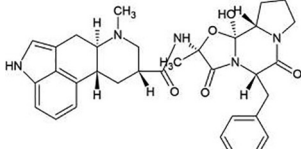
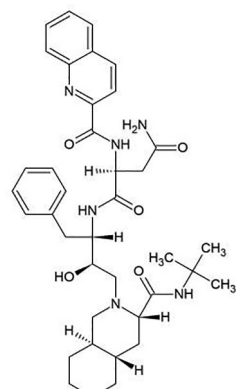
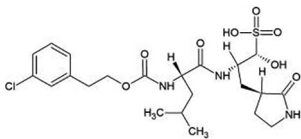
Fig. 2. Binding conformation and molecular interaction (compounds are represented as green sticks and key interacting residues are displayed in thin red wireframe representation) between SARS-CoV M^{Pro} lead compounds and. (A) Saquinavir (ZINC000026985532) (B) inhibitor SG85 (G85). The hydrophobic interactions are indicated by red arcs with radiating spikes and green dashed lines correspond to hydrogen bonds.

2.3. Evaluation of binding affinity of the compounds with the target enzymes

The binding affinity of each molecule along with the control inhibitors was evaluated against the three enzyme targets using

molecular docking approach. The binding sites for the compounds were defined by choosing grid box of dimensions of $25 \times 25 \times 25 \text{ \AA}^3$ with exhaustiveness value of 8 centred at $x:9.6421, y:-0.3396, z:18.3327$; $x:25.6069, y:44.4317, z:-5.6802$ and $x:-21.9764, y:24.4145, z:4.8599$ of SARS-CoV-2 M^{Pro},

Table 3
Binding energy scores and molecular interactions between top 5 leads and MERS-CoV M^{Pro}. The figures in bracket indicate the hydrogen bond length.

ZINC ID	Common Name	Structure	Binding Energy (kcal/mol)	Molecular Interactions	
				Hydrogen bonds	Hydrophobic interactions
ZINC000052955754	Ergotamine		-9.6	O3...SG(Cys148) [3.23 Å]	Met25, His41, Leu49, Leu144, Cys145, Met168, Glu169, Asp190, Lys191, Gln192, Val193 and His194 (N = 12)
ZINC000003860453	Ak-Fluor		-9.4	O2...NE2(His41) [3.01 Å] O5...O(Leu144) [3.23 Å] O5...NE2(His166) [3.20 Å] O5...OG(Ser147) [3.13 Å]	Met25, Phe143, Cys145, Gly146, Cys148, Gln167, Met168, Glu169, Lys191 and Gln192 (N = 10)
ZINC000003932831	Avodart		-9.3	Nil	His41, Leu49, Leu144, Cys145 Gln167, Met168, Glu169, Asp190, Lys191 and Gln192 (N = 10)
ZINC000003978005	Dihydroergotamine		-9.3	O1...SG(Cys145) [3.35 Å]	Met25, His41, Leu49, Leu144, Cys148, Met168, Glu169, Asp190, Lys191, Gln192 and His194 (N = 11)
ZINC000026664090	Saquinavir		-9.3	O2...SG(Cys145) [3.21 Å] O3...NE2(His41) [2.97 Å] N3...OE1(Gln192) [3.13 Å] N5...OE1 (Gln192) [2.99 Å] N4...O (Asp190) [3.18 Å]	Met25, Thr26, Leu49, Phe143, Leu144, Gly146, Ser147, Cys148, His166, Met168, Glu169 and Lys191 (N = 12)
Control (AW4)	GC813		-8.1	N13...O(Leu144) [2.80 Å] N13...OG(Ser147) [3.14 Å] O16...N(Ser147) [2.99 Å] O16...SG(Cys148) [3.17 Å] O16...N(Cys148) [3.10 Å] O16...N(Gly146) [3.26 Å] N03...OE1(Gln192) [2.80 Å]	Met25, His41, Leu49, Tyr54, Cys145, Met168, Glu169, Asp190, Lys191, Val193 and His194 (N = 11)

SARS-CoV M^{PRO} and MERS-CoV M^{PRO} respectively around the bound co-crystallized ligand. Autodock vina was used for performing molecular docking study which executes docking calculations based on sophisticated gradient optimization method (Trott and Olson, 2010).

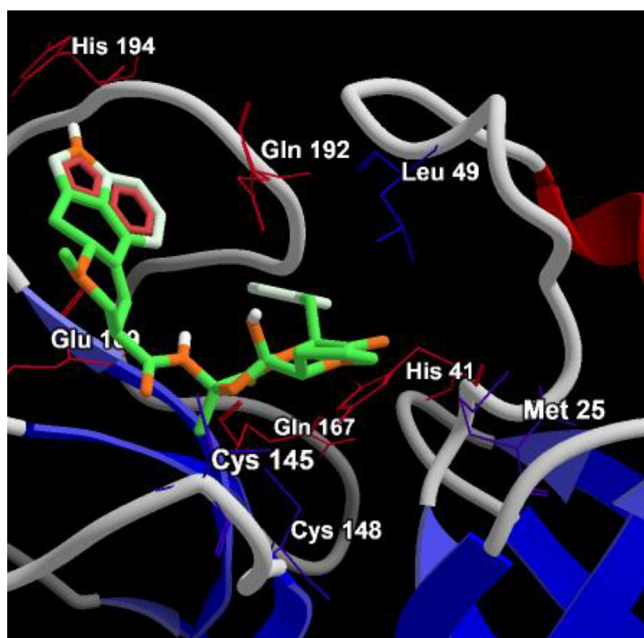
2.4. Evaluation of binding energy scores and study of binding poses

The lowest binding energy score of each ligand was taken into account for studying their binding poses. The molecular interactions (hydrogen bonds and hydrophobic interactions) between

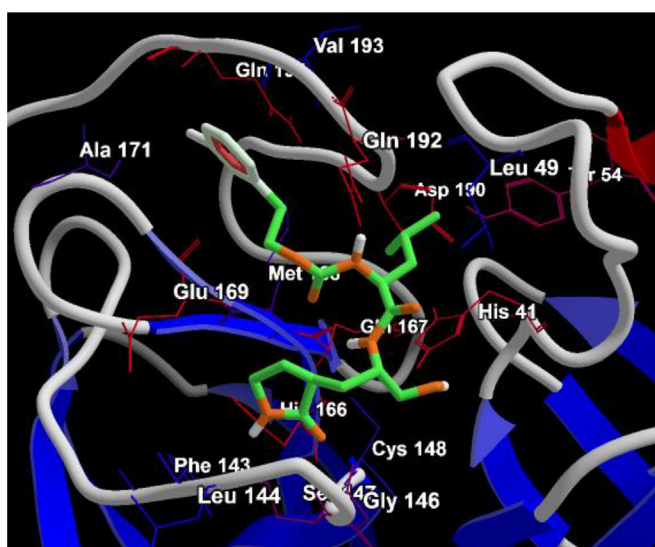
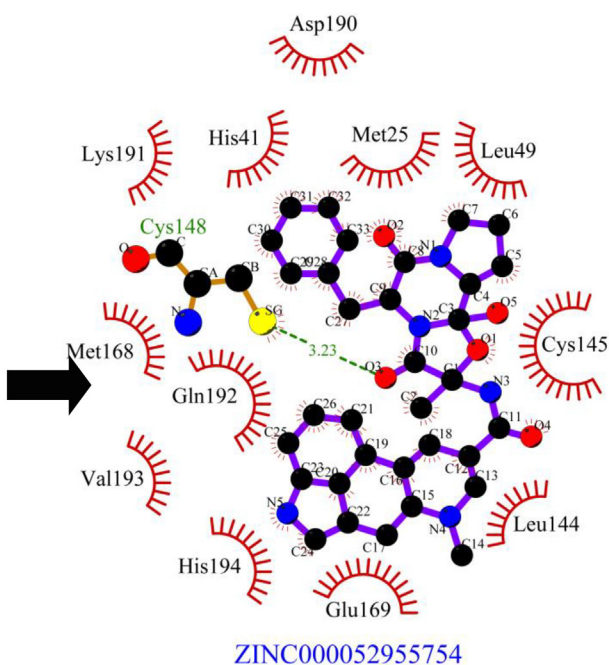
the target proteins and compounds were studied using LigPlot + version 1.4.5 tool (Laskowski and Swindells, 2011).

3. Results and discussion

The binding affinities of a total of 1390 FDA approved drugs were tested against three enzyme targets-SARS-CoV-2 M^{PRO}, SARS-CoV M^{PRO} and MERS-CoV M^{PRO}. The docking scores were benchmarked using three control inhibitors- α -ketoamide 13b (O6K), SG85 (G85) and GC813 (AW4). The top five lead molecules identified for SARS-CoV-2 M^{PRO} were Dihydroergotamine



(A)



(B)

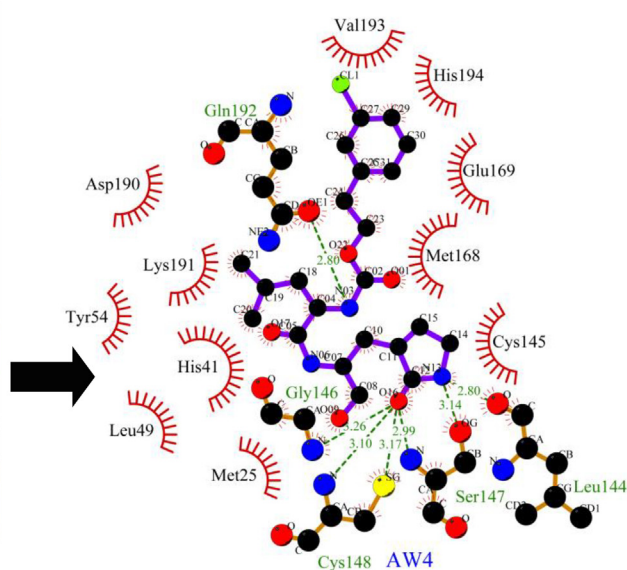


Fig. 3. Binding conformation and molecular interaction (compounds are represented as green sticks and key interacting residues are displayed in thin red wireframe representation) between MERS-CoV M^{PRO} and lead compounds and (A) Ergotamine (ZINC000052955754) (B) inhibitor GC813 (AW4). The hydrophobic interactions are indicated by red arcs with radiating spikes and green dashed lines correspond to hydrogen bonds.

(ZINC000003978005), Avodart (ZINC000003932831), Irinotecan (ZINC000001612996), Ergotamine (ZINC000052955754) and Oly-sio (ZINC000164760756) with binding energies of -9.4 kcal/mol, -9.3 kcal/mol, -9.3 kcal/mol and -9.2 kcal/mol respectively (Table 1). The best lead molecule Dihydroergotamine (ZINC000003978005) binds to a pocket within the Cys145-His41 dyad and exhibits two hydrogen bonds with backbone nitrogen (N) atom of Gly143 and the binding pose further shows the participation of nine residues (Thr25, His41, Cys44, Met49, Asn142, Cys145, His164, Met165 and Glu166) in hydrophobic interactions with SARS-CoV-2 M^{pro} (Fig. 1A). The control inhibitor, α -ketoamide 13b (O6K) scored binding energy of -6.9 kcal/mol with two hydrogen bonds—one with the side chain nitrogen (NE2) atom of His41 and the second one with the backbone nitrogen (N) atom of Glu166 and hydrophobic interactions via residues-Thr26, Met49, Cys145, His163, Met165, Pro168, Gln189 and Thr190 (Fig. 1B).

For the second target-SARS-CoV M^{pro}, the top 5 lead molecules identified were Saquinavir (ZINC000026985532), Ergotamine (ZINC000052955754), Nilotinib (ZINC000006716957), Raltegravir (ZINC000013831130) and Dihydroergotamine (ZINC000003978005) with binding energies of -9.6 kcal/mol, -9.5 kcal/mol, -9.4 kcal/mol, -9.2 kcal/mol and -9.2 kcal/mol respectively (Table 2). The best lead molecule-Saquinavir (ZINC000026985532) exhibits four hydrogen bonds (Three bonds with the backbone nitrogen (N) and oxygen (O) atom of Gly143, Leu141 and Glu166 and one hydrogen bond with side-chain oxygen (OE1) atom of Gln189) and twelve residues (Thr25, Thr26, His41, Met49, Phe140, Asn142, Cys145, His164, Met165, Leu167, Thr190 and Gln192) contributing to hydrophobic interactions with the target enzyme (Fig. 2A). The control, inhibitor SG85 (G85) of SARS-CoV M^{pro} exhibits binding energy of -7.9 kcal/mol with four hydrogen bonds (two hydrogen bonds with backbone N atoms of Cys145 and Glu166 and two hydrogen bonds with the side chain sulphur (SG) atom of Cys145 and side-chain oxygen (OE1) atom of Gln189) and hydrophobic interactions via sixteen residues (Thr25, Thr26, His41, Met49, Phe140, Leu141, Asn142, Gly143, Ser144, His163, His164, Met165, Asp187, Thr190, Ala191 and Gln192) (Fig. 2B).

The top 5 leads for the third target-MERS-CoV M^{pro} were found to be Ergotamine (ZINC000052955754), Ak-Fluor (ZINC000003860453), Avodart (ZINC000003932831), Dihydroergotamine (ZINC000003978005) and Saquinavir (ZINC000026664090) with binding energies of -9.6 kcal/mol, -9.4 kcal/mol, -9.3 kcal/mol, -9.3 kcal/mol and -8.1 kcal/mol respectively (Table 3). The best lead molecule- Ergotamine (ZINC000052955754) binds to a region within the Cys148-His41 catalytic dyad pocket and establishes one hydrogen bond with side chain sulphur (SG) atom of Cys148 and hydrophobic interactions with twelve important residues (Met25, His41, Leu49, Asp190, Leu144, Cys145, Met168, Glu169, Lys191, Gln192, Val193 and His194) (Fig. 3A). The control, inhibitor GC813 (AW4) shows binding energy of -8.1 kcal/mol with the target enzyme and the molecular interaction is reinforced by seven hydrogen bonds (four hydrogen bonds with the backbone atoms oxygen (O) atom of Leu144, nitrogen (N) atom of Ser147, nitrogen (N) atom of Gly146 and nitrogen (N) atom of Cys148 and three hydrogen bonds with side-chain oxygen (OG) atom of Ser147, sulphur (SG) atom of Cys148 and oxygen (OE1) atom of Gln192) and hydrophobic interactions via eleven residues- Met25, His41, Leu49, Tyr54, Cys145, Met168, Glu169, Asp190, Lys191, Val193 and His194 (Fig. 3B).

The molecules- Dihydroergotamine (ZINC000003978005) and Ergotamine (ZINC000052955754) were identified to be common leads interacting with all the three target enzymes with good binding energies and the favourable number of hydrogen bonds and hydrophobic interactions. Both Ergotamine and its derivative, Dihydroergotamine have been used in clinical practice for the treatment of acute migraine for many years. Both the drugs exhibit

complex modes of pharmacological binding with several receptors such as 5-HT (5-hydroxytryptamine), dopamine and noradrenaline receptors and are potent vasoconstrictors (Bigal and Tepper, 2003; Tfelt-Hansen et al., 2000).

4. Conclusion

Understanding the global health emergency and the immediate need for drugs and vaccines for the treatment of coronaviral infection, the present study is undertaken to identify promising inhibitors for main protease enzymes of coronaviruses through molecular docking approach. Our study suggests that anti-migraine drugs such as Ergotamine (ZINC000052955754) and its derivative, Dihydroergotamine (ZINC000003978005) are the most potent lead molecules which can be taken for further studies in wet lab experimentations.

Declaration of Competing Interest

The authors declare that they have no known competing financial interests or personal relationships that could have appeared to influence the work reported in this paper.

Acknowledgements

The authors would like to extend their sincere appreciation to the Deanship of Scientific Research at King Saud University for its funding of the research through the research group project #RG-1438-015. J. Lee thanks to Chungnam National University, Daejeon, Republic of Korea for the funding support. The authors thank the Deanship of Scientific Research and RSSU at King Saud University for their technical support.

References

- Anand, K., Ziebuhr, J., Wadhvani, P., Mesters, J.R., Hilgenfeld, R., 2003. Coronavirus main proteinase (3CLpro) structure: basis for design of anti-SARS drugs. *Science* (80) 300, 1763–1767.
- Bigal, M.E., Tepper, S.J., 2003. Ergotamine and dihydroergotamine: a review. *Curr. Pain Headache Rep.* 7, 55–62.
- Chan-Yeung, M., Xu, R.H., 2003. SARS: epidemiology. *Respirology* 8 (Suppl), S9–S14.
- Gentile, D., Patamia, V., Scala, A., Sciortino, M.T., Piperno, A., Rescifina, A., 2020. Putative inhibitors of SARS-CoV-2 main protease from a library of marine natural products: a virtual screening and molecular modeling study. *Mar. Drugs* 18, 225.
- Graham, R.L., Donaldson, E.F., Baric, R.S., 2013. A decade after SARS: strategies for controlling emerging coronaviruses. *Nat. Rev. Microbiol.* 11, 836–848.
- Gurung, A.B., Ali, M.A., Lee, J., Farah, M.A., Al-Anazi, K.M., 2020. Unravelling lead antiviral phytochemicals for the inhibition of SARS-CoV-2 Mpro enzyme through in silico approach. *Life Sci.* 117831.
- Gurung, A.B., Bhattacharjee, A., Ali, M.A., 2016. Exploring the physicochemical profile and the binding patterns of selected novel anticancer Himalayan plant derived active compounds with macromolecular targets. *Inform. Med. Unlocked* 5, 1–14.
- Halgren, T.A., 1996. Merck molecular force field. I. Basis, form, scope, parameterization, and performance of MMFF94. *J. Comput. Chem.* 17, 490–519. [https://doi.org/10.1002/\(SICI\)1096-987X\(199604\)17:5<490::AID-JCC1>3.0.CO;2-P](https://doi.org/10.1002/(SICI)1096-987X(199604)17:5<490::AID-JCC1>3.0.CO;2-P).
- Islam, R., Parves, R., Paul, A.S., Uddin, N., Rahman, M.S., Mamun, A. Al, Hossain, M.N., Ali, M.A., Halim, M.A., 2020. A molecular modeling approach to identify effective antiviral phytochemicals against the main protease of SARS-CoV-2. *J. Biomol. Struct. Dyn.* 1–20.
- Kandeel, M., Al-Nazawi, M., 2020. Virtual screening and repurposing of FDA approved drugs against COVID-19 main protease. *Life Sci.* 117627.
- Lai, M.M.C., Holmes, K.V., 2001. Coronaviridae: the viruses and their replication. In: Knipe, D.M., Howley, P.M. (Eds.), "Fields Virology". 4th. Lippincott, Williams & Wilkins, Philadelphia, pp. 1163–1185.
- Laskowski, R.A., Swindells, M.B., 2011. LigPlot+: multiple ligand-protein interaction diagrams for drug discovery. *J. Chem. Inf. Model.* 51, 2778–2786. <https://doi.org/10.1021/ci200227u>.
- Lee, H.-J., Shieh, C.-K., Gorbalenya, A.E., Koonin, E.V., La Monica, N., Tuler, J., Bagdzhadzhyan, A., Lai, M.M.C., 1991. The complete sequence (22 kilobases) of murine coronavirus gene 1 encoding the putative proteases and RNA polymerase. *Virology* 180, 567–582.
- Lobo-Galo, N., Terrazas-López, M., Mart'inez-Mart'inez, A., D'iaz-Sánchez, Á.G., 2020. FDA-approved thiol-reacting drugs that potentially bind into the SARS-CoV-2 main protease, essential for viral replication. *J. Biomol. Struct. Dyn.* 1–12.

- O'Boyle, N.M., Banck, M., James, C.A., Morley, C., Vandermeersch, T., Hutchison, G.R., 2011. Open babel: an open chemical toolbox. *J. Cheminform.* 3, 33. <https://doi.org/10.1186/1758-2946-3-33>.
- Richman, D.D., Whitley, R.J., Hayden, F.G., 2016. *Clinical virology*. John Wiley & Sons.
- Singhal, T., 2020. A review of coronavirus disease-2019 (COVID-19). *Indian J. Pediatr.* 87, 281–286. <https://doi.org/10.1007/s12098-020-03263-6>.
- Snijder, E.J., Spaan, W.J.M., 1995. The coronaviruslike superfamily. In: *The Coronaviridae*. Springer, pp. 239–255.
- Sterling, T., Irwin, J.J., 2015. ZINC 15–ligand discovery for everyone. *J. Chem. Inf. Model.* 55, 2324–2337.
- Tahir ul Qamar, M., Alqahtani, S.M., Alamri, M.A., Chen, L.-L., 2020. Structural basis of SARS-CoV-2 3CLpro and anti-COVID-19 drug discovery from medicinal plants. *J. Pharm. Anal.* <https://doi.org/10.1016/j.jpha.2020.03.009>.
- Tfelt-Hansen, P., Saxena, P.R., Dahlöf, C., Pascual, J., Lainez, M., Henry, P., Diener, H.-C., Schoenen, J., Ferrari, M.D., Goadsby, P.J., 2000. Ergotamine in the acute treatment of migraine: a review and European consensus. *Brain* 123, 9–18.
- Trott, O., Olson, A.J., 2010. AutoDock Vina: improving the speed and accuracy of docking with a new scoring function, efficient optimization, and multithreading. *J. Comput. Chem.* 31, 455–461. <https://doi.org/10.1002/jcc.21334>.
- Wang, C., Horby, P.W., Hayden, F.G., Gao, G.F., 2020. A novel coronavirus outbreak of global health concern. *Lancet* 395, 470–473.
- Xue, X., Yu, H., Yang, H., Xue, F., Wu, Z., Shen, W., Li, J., Zhou, Z., Ding, Y., Zhao, Q., et al., 2008. Structures of two coronavirus main proteases: implications for substrate binding and antiviral drug design. *J. Virol.* 82, 2515–2527.
- Yang, H., Yang, M., Ding, Y., Liu, Y., Lou, Z., Zhou, Z., Sun, L., Mo, L., Ye, S., Pang, H., et al., 2003. The crystal structures of severe acute respiratory syndrome virus main protease and its complex with an inhibitor. *Proc. Natl. Acad. Sci.* 100, 13190–13195.
- Ziebuhr, J., Snijder, E.J., Gorbalenya, A.E., 2000. Virus-encoded proteinases and proteolytic processing in the Nidovirales. *J. Gen. Virol.* 81, 853–879.